On the Very High Energy Confinement Observed in Super H-mode DIII-D Experiments

S. Ding[1,2,*], A. M. Garofalo[3], M. Knolker[1], A. Marinoni[4], J. McClenaghan[3] and B. A. Grierson[5]

[1]Oak Ridge Associated Universities, Oak Ridge, TN 37831, USA
[2]Institute of Plasma Physics, Chinese Academy of Sciences, P. O. Box 1126, Hefei, Anhui, 230031, China
[3]General Atomics, P. O. Box 85608, San Diego, California, 92186-5608, USA
[4]Plasma Science and Fusion Center, Massachusetts Institute of Technology, Cambridge, Massachusetts, 02139, USA
[5]Princeton Plasma Physics Laboratory, Princeton University, Princeton, New Jersey, 08543, USA

E-mail: `dingsiye@fusion.gat.com`

Abstract. Analysis of recent super H-mode experiments on DIII-D shows that high rotation, not high pedestal, plays the essential role in achieving very high confinement $H_{98y2} > 1.5$. Very high confinement is reached early on in the H-mode phase of these discharges, when the pedestal is still very low, but after the toroidal rotation has already built-up to very high levels in the core. As the discharge evolves, the rotation drops, and so does the energy confinement, despite a sustained very high pressure pedestal. During this evolution, the confinement quality is linearly correlated with the core toroidal rotation, which varies according to different levels of injected neutral beam torque per particle. Core transport modeling shows that the contribution from rotation in the $E \times B$ shear is responsible for confinement quality significantly in excess of standard H-mode ($H_{98y2} \sim 1$).

PACS numbers: 52.55.Fa, 52.25.Fi

1. Introduction

The importance of pedestal parameters, especially the pedestal height, in tokamak plasmas is well-documented [1]. Assuming stiffness in the temperature profiles, the plasma performance, including stored energy, β, etc., becomes largely determined by the pedestal height, which sets the boundary conditions for the core in H-mode plasmas without internal transport barriers [1]. With fixed profile shape/radial gradients (temperature, density), the higher the pedestal pressure is, the higher the plasma stored energy will be. Furthermore, at fixed injected power and other major parameters, the higher the plasma stored energy is, the higher the confinement quality will be. This is how the confinement is tightly connected with pedestal height.

Good confinement is important for an economical fusion reactor design. For example, one can see from the energy confinement quality factor, $H_{98y2} = \tau_E/\tau_{E,98y2} \sim W/P^{0.31}$ (where W is the stored energy and P is the injected power), that if the H factor drops from 1.5 (advanced tokamak, AT) to 1.0 (standard H-mode), the required injected power will have to be at least three times higher in order to keep the same stored energy or fusion power. In projection to ITER and future reactors that assumes stiff core profiles, the fusion power is predicted to scale with square of pedestal pressure [2]. Therefore, the realization of super H-mode is a significant advance on the high pedestal path towards higher plasma performance [3, 4].

The super H-mode regime was first predicted using the EPED model, which calculates critical constraints for peeling-ballooning and kinetic ballooning stability, and combines them to predict the pedestal height and width [7]. Then, based on a quiescent H-mode edge, super H-mode experiments on DIII-D discovered a path with strong plasma shaping at high density, leading to a doubling of the edge pressure over the standard H mode at these parameters [3], although only transiently. So far, the bifurcated state ('channel') of super H-mode in the Peeling-Ballooning boundary has, only been obtained transiently ($\sim \tau_E$). In the best cases, the plasma pedestal can be maintained somewhere 'near' the access to the bifurcation, still characterized by a significant pedestal height. Thus, in the following, the phrase "super H-mode plasmas" will be used in general to indicate plasmas obtained in experiments that explore operation in and near the super H channel. These plasmas often have good confinement exceeding standard H-mode, i.e. $H_{98y2} > 1.0$. It was initially believed that the very high thermal energy confinement was enabled by the large pedestal height [4].

In this paper, analysis of recent super H-mode experiments on DIII-D shows that rapid plasma rotation, not high pedestal, yields the very high thermal energy confinement ($H_{98y2} > 1.5$). The causality can be inferred based on: 1) The high confinement phase starts at very low pedestal pressure, but follows the build-up of very high core rotation; 2) Different levels of rotation correlate with different levels of injected torque per particle; 3) Transport modeling shows that without the contribution of rotation in the $E \times B$ shear, the predicted confinement quality is significantly reduced in agreement with the empirical observations at lower rotation. The physical mechanism,

we believe, is related with the critical gradient shifted by large $E \times B$ shear, which was discussed in early studies [5, 6].

2. Confinement quality not correlated with pedestal height

This section gives an overview of the set of discharges analyzed in this paper, and shows that the evolution of these typical super H-mode experiments follows this pattern: high external torque per particle, high toroidal rotation, low pedestal and high energy confinement in the early period of the H-mode phase; lower external torque per particle, lower toroidal rotation, higher pedestal but lower energy confinement in the later period of the H-mode phase.

These recent super H-mode experiments on DIII-D extended the experimental strategy from previous counter-neutral beam injection (NBI) quiescent H-mode edge to ELMing edge using co-NBI at full magnetic field (B_{T}=2.1–2.2 T) and high current (I_{p}=1.4–2.0 MA). High plasma performance and pedestal parameters are achieved in these discharges [8]. Because of the variable co-NBI torque in these experiments, it is possible to investigate the effect of plasma rotation on thermal energy confinement in super H-mode plasmas.

The above pattern is shown in the time history of typical discharges in the recent super H-mode experiments on DIII-D in figure 1. Soon after the plasma reaches its plasma current flattop at 1.4 s, the injected NBI power increases from 1.2 to 6.5 MW at 1.5 s. The plasma toroidal rotation increases rapidly. It reaches its maximum value at around 2.0 s, when a small $n = 3$ field is applied to mitigate the ELMs. Then the rotation decreases until a stationary value is reached around $t = 2.5$ s. This stationary value is mainly determined by the injected torque per particle, as shown in figure 1(e) and discussed in more detail later. Since the plasma current and the average density vary somewhat ($\leq 25\%$) within this group of discharges, the normalized energy confinement to scaling laws is taken as a measure of confinement quality. The energy confinement quality factors, both for thermal energy ($H_{98\mathrm{y2}}$) and total energy ($H_{89\mathrm{p}}$), follow the trend of toroidal rotation very well in figure 1. The confinement calculation takes into account the heating power (Ohmic, NBI), stored energy (including a calculation of the fast-ion fraction) and time evolution of the stored energy ($\mathrm{d}W/\mathrm{d}t$), i.e. $\tau_{\mathrm{E}} = W/(P - \frac{\mathrm{d}W}{\mathrm{d}t})$. Surprisingly, confinement does not correlate with pedestal height (figure 1(a)). Very high confinement ($H_{98\mathrm{y2}} > 1.5$) is reached with low pedestal pressure at around 2.0 s. Note that the typical electron pressure at pedestal is about $5 - 6$ kPa for standard H-mode on DIII-D. When confinement drops with toroidal rotation later, the pedestal height is sustained at a high level (around 10 kPa of electron pressure). For the cases with standard (low) rotation (about 70 km/s) at $\rho = 0.4$, $H_{98\mathrm{y2}}$ is around 1.0. At this low rotation these high pedestal super H-mode discharges have lost most of the confinement quality in excess of standard H-mode. For reference, note that the volume average rotation predicted for ITER is less than 25 km/s, shown in figure 1(d) by the dashed line [9].

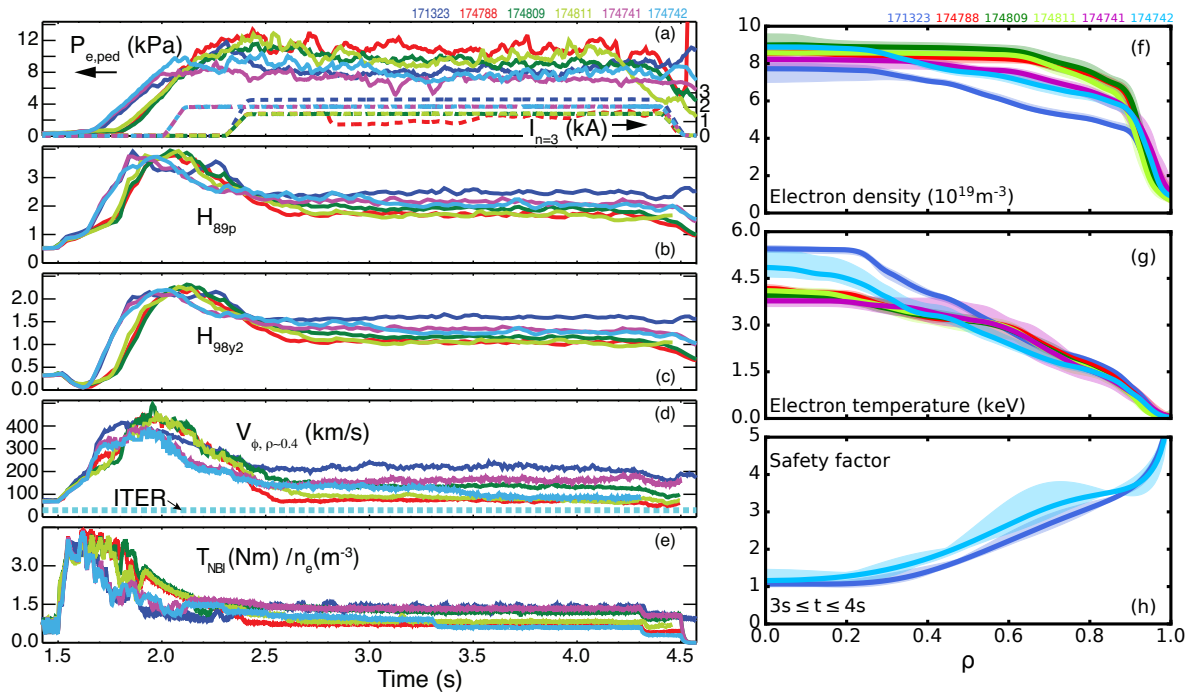

Figure 1. Time histories of super H-mode discharges: (a) Solid lines are electron pedestal pressure from tanh fit; Dashed lines are the current waveforms for $n = 3$ magnetic perturbation coils; (b) $H_{89\mathrm{p}}$; (c) $H_{98\mathrm{y2}}$; (d) toroidal rotation at $\rho = 0.4$; Cyan dashed line shows the ITER prediction of toroidal rotation [9]; (e) NBI torque per particle, with n_e the line averaged electron density (10 ms smoothing); (f) electron density profiles; (g) electron temperature profiles and (h) safety factor profiles between 3 and 4 s. Solid line shows the averaged value and the shaded region represents the error bar.

Figure 1(f), (g) and (h) show the electron density, temperature and safety factor profiles (q profiles) for the discharges investigated in this work. The averaged period is from 3 to 4 s. The variation of electron density and temperature for each discharge during this period is small, while there are some differences between discharges. In terms of collisionality, the change is at most about a factor of 2. The q profiles are from equilibrium reconstructions including motional Stark effect (MSE) measurements of the magnetic field pitch angle radial profile. There are only two discharges with MSE data among the six discharges analyzed in this paper.

The surprising behavior of the confinement quality relative to the pedestal height is visualized in more details in figure 2, where the evolution for one of the discharges in figure 1 is plotted in an expanded time range around the L-H transition. The maximum energy confinement is obtained with very low pedestal at $t \sim 1.75$ s, but follows a strong rotation build-up. Very peaked profiles of rotation and ion temperature are measured at this time, showing that good confinement is clearly driven by the core. The ion pedestal temperature (1.8 keV) is low at this time compared with that at later time (3.3 keV at $t \sim 2.0$ s).

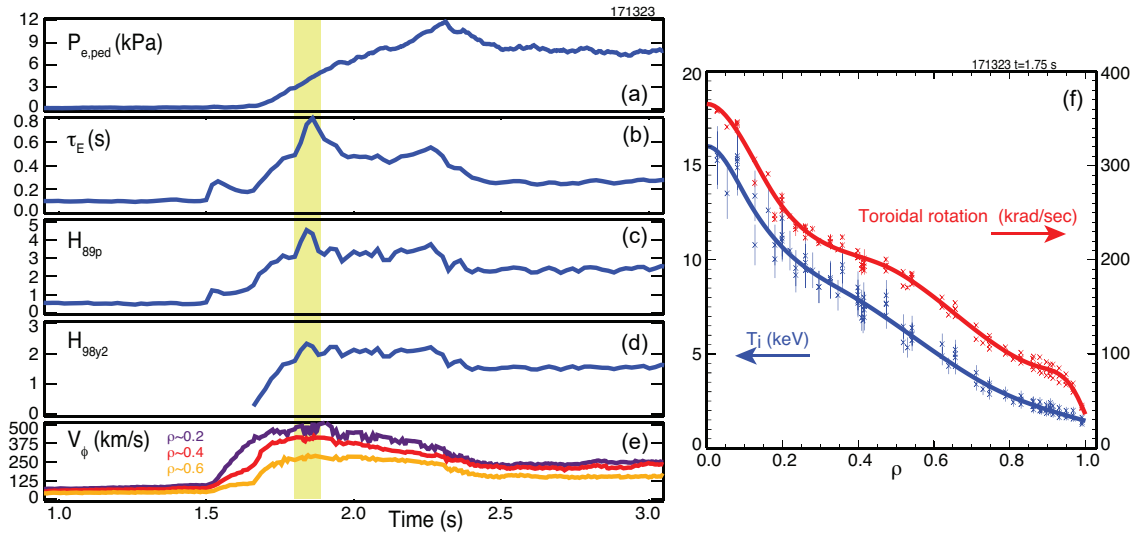

Figure 2. Time histories of (a) electron pedestal pressure ($P_{\mathrm{e,ped}}$); (b) energy confinement time; (c)-(d) energy confinement factors, $H_{89\mathrm{p}}$, $H_{98\mathrm{y2}}$ and (e) toroidal rotation, V_ϕ at different radial positions in an expanded time range around the L- to H-mode transition for one of the discharges in figure 1 (171323). The vertical band indicates the time slice for profiles in (f): ion temperature (in blue) and toroidal rotation (in red).

3. Confinement quality linearly correlated with core toroidal rotation

In figure 3, the trajectories of several super H-mode discharges show that the confinement is linearly correlated with the toroidal rotation in the core. The faster the plasma rotates, the higher is the energy confinement. Meanwhile, the pedestal pressure acts in a pretty constant way during the most change of toroidal rotation in figure 3(a). Note that, even beyond the set of discharges analyzed in this paper, there is no experimental observation of very high confinement ($H_{98\mathrm{y2}} > 1.5$) at low rotation, e.g. $V_{\phi,\rho\sim0.4} < 100$ km/s in any DIII-D super H-mode experiments to date. This correlation between thermal energy confinement and toroidal rotation is very similar to what is found in the DIII-D advanced inductive scenario, which is typically characterized by high normalized fusion performance at high rotation, but suffers confinement degradation at low rotation [10].

Note how figure 3 also shows that, for given rotation, the same H_{98} is obtained with significantly different pedestal heights. For example, comparing discharges 174788 and 171323 at the same rotation $V_\phi \sim 230$ km/s, the pedestal is 50% higher in 174788 (shown in figure 3(a)). Consistent with what one might expect, the stored energy also is 50% higher in 174788, which is 2.69 MJ versus 1.78 MJ (171323). However, H_{98} is the same for the two cases (shown in figure 3(b)). This is because other parameters have to be different for the two discharges to have different pedestal. In this case, I_p is 24% higher, density is 15% higher and P_inj is 13% higher in 174788.

Most of the discharges shown in figure 3 have an $n = 2$ rotating mode with fairly large saturated amplitude. It is observed that the amplitude of $n = 2$ mode is higher

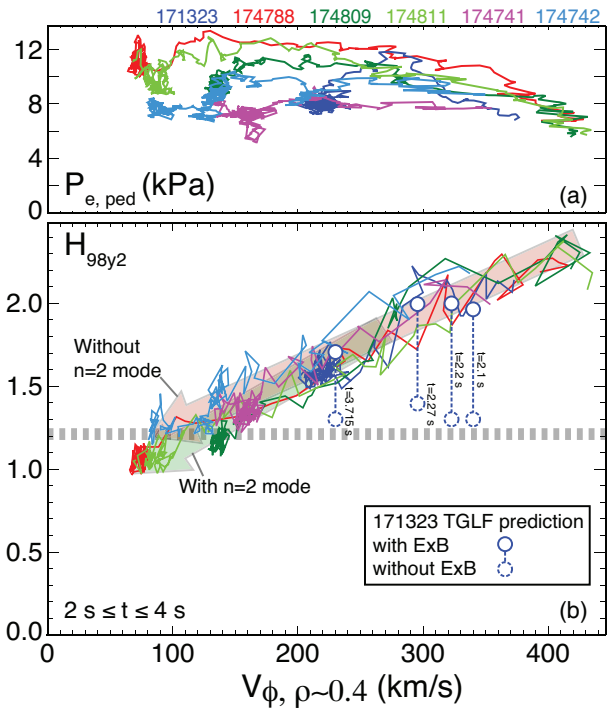

Figure 3. (a) Correlation between electron pedestal pressure and toroidal rotation at $\rho = 0.4$ for super H-mode discharges of figure 1 in time range from 2.0 to 4.0 s. (b) Correlation between energy confinement factor (H_{98y2}) and toroidal rotation. Light orange and light green arrows point to different low-rotation limits of H_{98y2}, depending on presence of $n = 2$ tearing mode. Blue circles are the H_{98y2} from TGLF predictions with and without $E \times B$ rotational shear effects for discharge 171323 at different times. Dashed line is the empirical low-rotation H_{98y2} without $n = 2$ tearing mode.

when the toroidal rotation becomes lower, which may be responsible for a stronger confinement deterioration with lower rotation. This also is similar to the phenomenon reported in the analysis of advanced inductive plasmas on DIII-D [10, 11].

Two exceptions are discharges 171323 and 174742. These discharges have no $n = 2$ mode, thus enabling a quantification of the effect of the $n = 2$ mode on the confinement degradation as the rotation drops, indicated by the diverging arrows in figure 3. An estimation of the island width with high experimental $\delta B_{\mathrm{n=2}}$ amplitude gives $\sim 9.3 \pm 2.3$ cm. The effect of this island width on the energy confinement is estimated by using the "belt model" [12]. The model predicts about $13 \pm 2.5\%$ reduction of energy confinement. This is in good agreement with the empirical observed difference between "without $n = 2$ mode" and "with $n = 2$ mode" discharges. The simple extrapolation suggests that super H-mode may still have slightly better thermal energy confinement than standard H-mode in very low reactor relevant rotation, if no saturated tearing mode is present. Transport analysis supports this assessment, as discussed later and also summarized in figure 3.

4. Toroidal rotation correlated with injected torque per particle

Since toroidal rotation correlates well with thermal energy confinement in these super H-mode plasmas, here we discuss what causes the rotation changes in the experiments. An important factor is the change of external momentum source (the actuator) during the rotation change. In the time histories shown in figure 1(d), the toroidal rotation starts to increase promptly as is expected for the response of a low density plasma to strong neutral beam torque injection starting at t=1.5 s.

As the density builds up after the L- to H-mode transition ($t \sim 1.7$ s), the NBI torque per particle (figure 1(e)) decreases, causing the rotation to reach a maximum and then decrease ~ 300 ms later. Around this time ($t \sim 2.0$ s) a small $n = 3$ field is applied for ELM mitigation, causing an additional rotation drop. The NBI torque per particle and the toroidal rotation reach stationary levels after $t \sim 2.5$ s.

The levels of toroidal rotation in the stationary phase are well correlated with the levels of injected torque per particle, for a similar saturated amplitude of $n = 2$ tearing mode, as shown in figure 4(a). It is well known that a tearing mode rotating with the plasmas, can exert a significant drag on the plasma rotation by interacting with the eddy currents generated on the surrounding resistive wall [13]. The slope of the dash line in figure 4(a) is representative of the angular momentum confinement time (τ_ϕ). Three discharges with large saturated $n = 2$ mode amplitude (174788, 174809, 174811, figure 4(c)) have the same τ_ϕ.

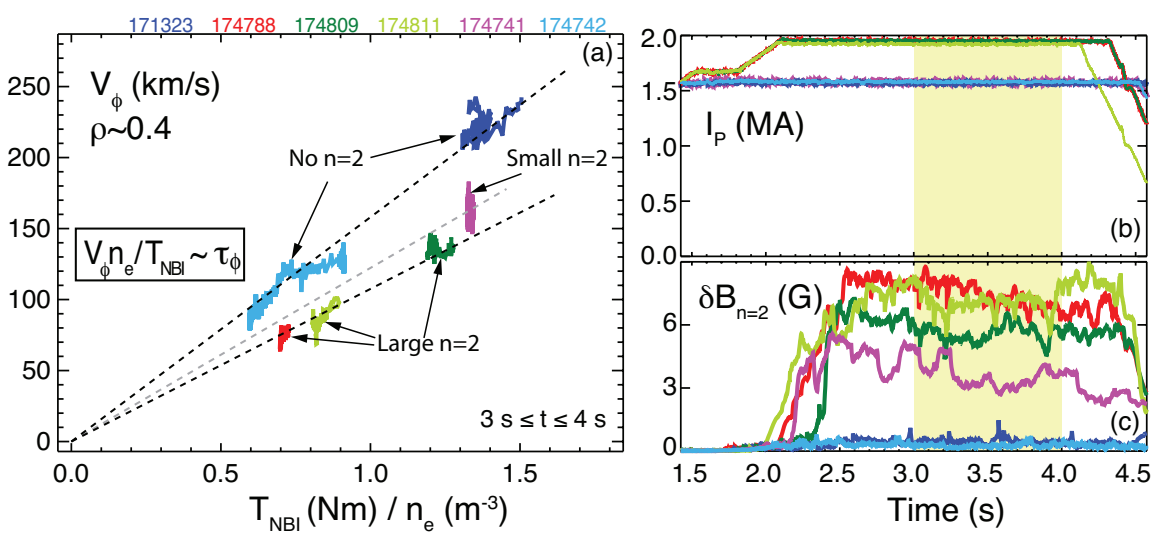

Figure 4. (a) Correlation between toroidal rotation (at $\rho = 0.4$) and NBI torque per particle. Time window for all discharges is between 3 and 4 s (stationary phase). Slope of the dashed lines is proportional to the angular momentum confinement time. (b) Plasma current. (c) Amplitude of $n = 2$ core tearing mode measured at the wall. Highlighted region shows the time window for data shown in (a).

The three other discharges have lower plasma current (171323, 174741, 174742, figure 4(b)), which should work to lower τ_ϕ; however, discharges 171323 and 174742

have no $n = 2$ mode while discharge 174741 has a small amplitude $n = 2$ mode. The fact that τ_ϕ is higher in figure 4(a) for the three lower current discharges indicates that the drag from the $n = 2$ mode has a significant effect on τ_ϕ. The rotation has a simple linear dependence on the NBI torque per particle, once the $n = 2$ mode amplitude is taken into consideration.

5. Confinement quality not correlated with temperature ratio $T_\mathrm{i}/T_\mathrm{e}$

The analysis in this section shows that a change of $T_\mathrm{i}/T_\mathrm{e}$ during discharge evolution does not contribute to the confinement change in our dataset of super H-mode discharges. $T_\mathrm{i}/T_\mathrm{e}$ is usually an important parameter in the turbulence and transport study because it affects the expected growth rate of ion and electron temperature gradient modes (ITG, ETG) as well as the critical electron and ion temperature gradients length $L_\mathrm{Ti,e}$, where $R/L_\mathrm{Ti,e} \sim 1 + T_\mathrm{i,e}/T_\mathrm{e,i}$ [14, 15, 16, 17]. One should switch label 'i' and 'e' for switching instability between ITG and ETG. Once the profiles exceed the critical gradients, turbulence will be provoked to drive large heat transport resulting in the phenomenon of profile resilience.

When $T_\mathrm{i}/T_\mathrm{e}$ changes, the critical gradient changes as well as the observed transport and overall confinement. When examining the stationary phase (3.0–4.0 s) of the discharges in the dataset shown in figure 1, clear proportional trend in H_98y2 vs toroidal rotation can be seen in figure 5(a) among all the discharges in the dataset.

Figure 5(b) shows that $T_\mathrm{i}/T_\mathrm{e}$ near mid-radius ($\rho = 0.4$) stays quite constant despite the different toroidal rotation at the same radial position and different overall confinement quality. The average $T_\mathrm{i}/T_\mathrm{e}$ value at $\rho = 0.4$ is about 1.6 for the discharges in this dataset, indicating that $T_\mathrm{i}/T_\mathrm{e}$ in the plasma core has no role in the change of thermal confinement during the stationary phase of these discharges.

Similarly, figure 5(d) shows the generally constant $T_\mathrm{i}/T_\mathrm{e}$ ratio evaluated at the top of the pedestal over a wide range of pedestal toroidal rotation and in an even broader time window (2.0–4.0 s). Only one discharge (174741) has large variation in $T_\mathrm{i}/T_\mathrm{e}$ at the pedestal, but no corresponding variation in H_98y2 can be found at the same toroidal rotation. Instead, H_98y2 has a proportional relation to the pedestal toroidal rotation (figure 5(c)), similar to that discussed earlier for the core rotation.

The data presented here strongly suggests that the physics of $T_\mathrm{i}/T_\mathrm{e}$ is not responsible for the thermal energy confinement degradation observed during the time evolution of these super H-mode discharges. Another investigation using transport modeling of these super H-mode plasmas presented in reference [8] also indicates that the plasma is barely responsive to temperature variations near the experimental conditions.

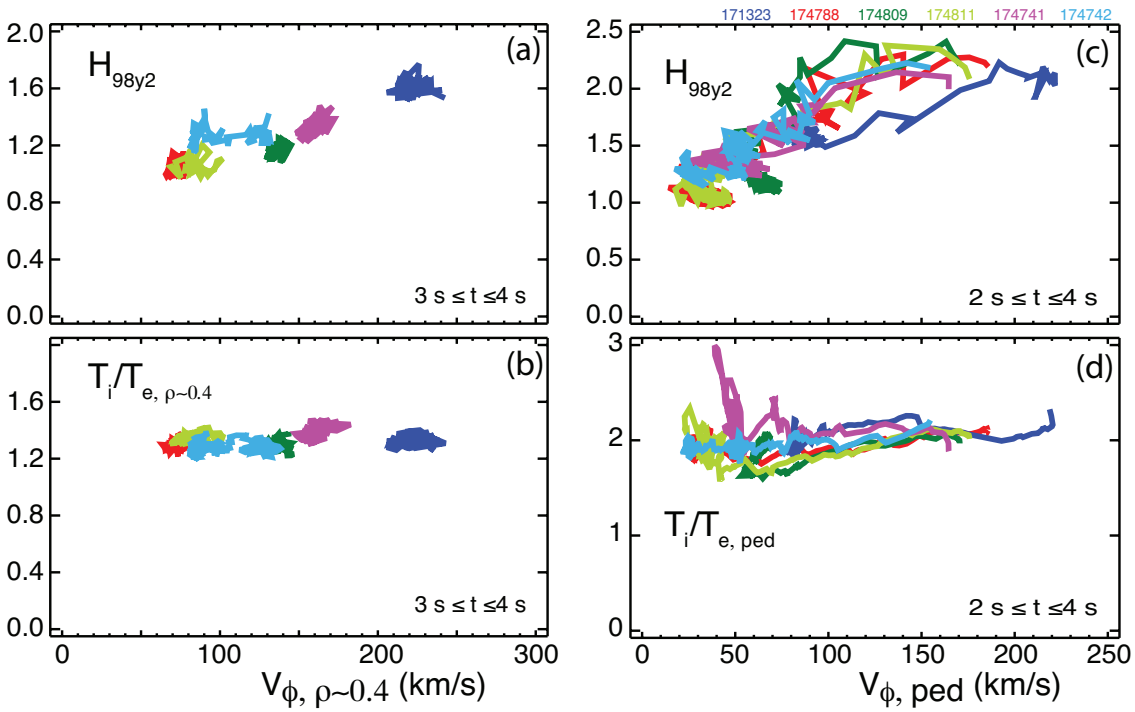

Figure 5. The correlation between H_{98y2}, T_i/T_e and toroidal rotation in the super H-mode dataset showed in figure 1. (a)–(b)T_i/T_e and toroidal rotation measured at mid-radius, $\rho = 0.4$. Time window is between 3.0 to 4.0 s; (c)–(d) T_i/T_e and toroidal rotation measured at pedestal top ($\rho = 0.8$). Time window is between 2.0 to 4.0 s.

6. Gyrofluid transport modeling of the role of $E \times B$ turbulence stabilization

Transport modeling shows that a good match of the experimental observations can be achieved by including the toroidal rotation and related $E \times B$ shear, but the predicted plasma performance would be significantly below experimental observations if the effects of toroidal rotation were not considered. The simulations predict temperature profiles by using transport solver TGYRO [18], which utilizes TGLF [19] for turbulence transport, NEO [20] for neoclassical transport and is integrated into the OMFIT framework [21]. For the results showed in this paper, we choose to hold the density fixed to the experimental profile in order to show the impact on the temperature profiles. Note that when density is also evolved, the impact on energy confinement is the same, although the predicted temperature profiles will change. The simulation domain is from ρ =0.2 to 0.8. The saturation rule used in TGLF is SAT1 [22].

As shown in figure 6, the simulation with full $E \times B$ can reproduce the temperature profiles for super H-mode discharge 171323 at 3.715 s, which has a high confinement corresponding to $H_{98y2} \sim 1.6$ or $H_{89p} \sim 2.5$. The ion temperature is slightly over-predicted by TGYRO in the core, resulting in a predicted $H_{98y2} \sim 1.7$, slightly above the experimental value. Turning off the $E \times B$ shear physics, or leaving only the ∇p contribution in the $E \times B$ term, leads to a significant drop in the predicted profiles. The

temperature reduction that results from removing the $E \times B$ effect in the simulation is calculated to decrease H_{98y2} from 1.7 to 1.3.

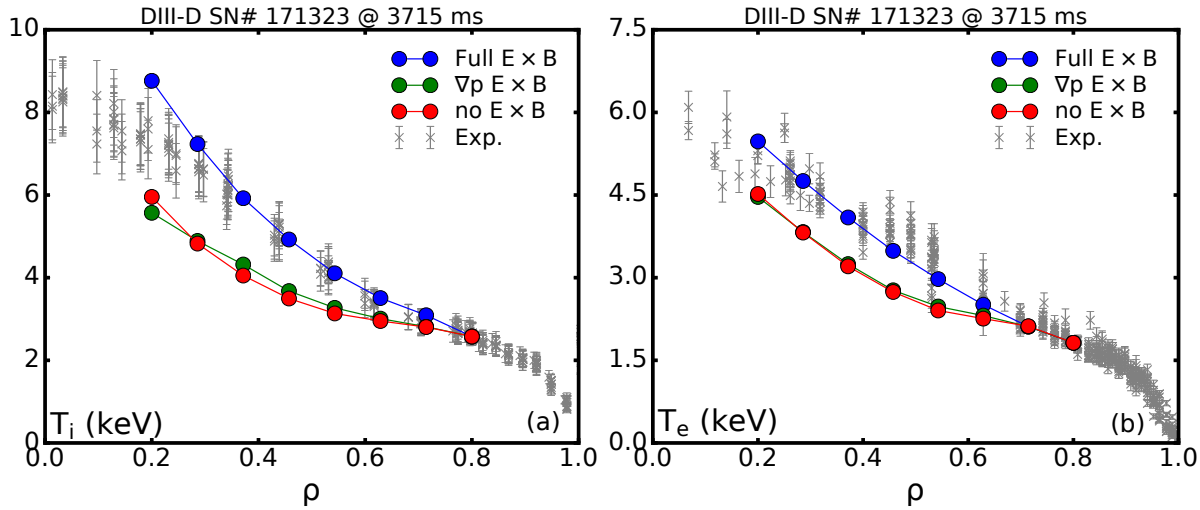

Figure 6. Predicted temperature profiles in TGYRO simulations. (a) Ion temperature; (b) electron temperature. Simulation results with different colors indicate the different treatment of $E \times B$ shear physics. Blue for full $E \times B$; green for ∇p $E \times B$ only; red for no $E \times B$. In gray are the experimental measurements for super H-mode discharge 171323 at 3.715 s.

Similar analysis was repeated for several other time slices in the same discharge, and all the results are illustrated in figure 3, showing a similar prediction of the energy confinement without rotation, for time slices with different experimental confinement values. Note that for the analysis times earlier in the H-mode phase, the experimental toroidal rotation is much higher. Correspondingly, the confinement quality with experimental rotation is much higher ($H_{98y2} > 2.0$), but the decrease in H_{98y2} due to the reduction of predicted temperatures from removing the $E \times B$ effect in the simulation is much larger, leading to approximately the same confinement quality predicted without $E \times B$ effect for all analysis times, irrespective of the starting experimental rotation. This confirms that the rotation governs the energy confinement throughout the entire time range (2.0–4.0 s) shown in figure 3. A relatively small effect of the pedestal height can be seen in the slightly higher $H_{98y2} \sim 1.4$ predicted with no $E \times B$ effect for the time $t = 2.27$ s, since this time-slice corresponds to the peak pedestal height, and is the only time when the pedestal is actually inside the super H-mode channel.

Overall, these transport simulations confirm the importance of toroidal rotation for the thermal energy confinement in these super H-mode experiments, and support the empirical extrapolation that discharges with "near super H-mode" pedestal at low $E \times B$ shear and without $n = 2$ mode have only modestly enhanced confinement with $H_{98y2} \sim 1.2$. Alcator C-Mod achieved the world record pedestal pressure using super H-mode approach without NBI torque. The two representative discharges discussed in reference [23] have H_{98y2} around 1.2–1.3, which is consistent with the no-rotation

prediction of DIII-D super H mode plasma in this paper.

Simulations of different pedestal heights are also performed. Pedestal ion and electron temperatures (boundary conditions of TGYRO modeling) receive different multiplier in different cases at constant pedestal density. The range of multiplier is from 0.5 to 1.3 in the test. The results of the simulations show: (1) If the temperature boundary conditions are increased or decreased, the predicted temperature profiles move up or down accordingly. Therefore, higher pedestal gives higher stored energy, which is consistent with the experimental observation, discussed about figure 3; (2) A reduction of stored energy around 25% is observed in all cases (including the original case with un-scaled pedestal height), when $E \times B$ shear effect is turned off. This suggests that $E \times B$ shear plays similar role in super H-mode plasma regardless of the variation of pedestal height with the assumption of unchanged rotation.

One can see that there are differences in the experimental profiles for the discharges in this database (figure 1(f)-(h)). Beside the effect of toroidal rotation analyzed in this work, other effects, such as collisionality, magnetic shear and fast ion stabilization [24] can also contribute to the observed differences in the confinement. These could be interesting topics for future work.

Regarding the dominant micro-instability in super H core plasma, gyrofluid simulation suggests a low-k ion mode. However, gyrokinetic simulations are not performed in this work. Therefore, it is a worthy future study to understand whether the dominant micro-instability changes or not between different states in each discharge or different discharges by gyrokinetic analysis. There might be different dominant instabilities that drive the anomalous transport. Those instabilities might be stabilized by $E \times B$ shear at different rates, which might be a plausible mechanism for the observed dependencies.

7. Summary

In summary, in the recent super H-mode experiments on DIII-D, it is observed that a very high thermal energy confinement quality ($H_{98y2} > 1.5$) does not correlate with the pedestal height. Very high confinement quality is reached soon after the L-H transition with very low pedestal pressure. As the discharge evolves, the confinement drops as the rotation drops, despite sustained very high pedestal. The energy confinement quality is linearly correlated with the core toroidal rotation (thus core rotation shear).

Beyond a simple correlation, causality can actually be inferred based on: 1) The high confinement phase follows the build-up of very high core rotation (thus high core rotation shear); 2) Different levels of rotation correlate with different levels of injected torque per particle at similar $n = 2$ mode amplitude, i.e. the decrease of toroidal rotation is mainly the result of change in external actuator; 3) Transport modeling shows that without the contribution of rotation in the $E \times B$ shear, confinement quality in excess of standard H-mode will significantly reduce.

The analysis also shows that the physics of critical gradient change due to different

T_i/T_e in the turbulence transport is not responsible for this phenomenon. The trend we report in this paper suggests that these super H-mode plasmas lose their attractive very high thermal energy confinement, despite possessing a high pedestal pressure, with standard toroidal rotation at mid-radius. Super H-mode plasma is still expected to possess slightly higher thermal confinement than standard H-mode ($H_{98y2} \sim 1.2$). However, experiments have shown that the presence of $n = 2$ mode could further reduce the thermal confinement to standard H-mode level or even lower when extrapolating to reactor relevant rotation. Further studies on how to improve the energy confinement at low rotation will be key to the development of super H-mode scenario for a high performance fusion reactor. The differences in other physical factors, such as collisionality, magnetic shear and fast ion stabilization, can also contribute to the observed differences in the confinement. Detailed investigation on the roles of these factors could be interesting topics for future work.

Acknowledgments

The authors would like to thank the OMFIT group for their support in performing the transport simulations. The authors also thank Dr. Tom Osborne (General Atomics) for help on equilibrium reconstruction and Dr. Xiang Jian (University of California, San Diego) for discussion on the effects of various physical factors on confinement. This material is based upon work supported by the U.S. Department of Energy, Office of Science, Office of Fusion Energy Sciences, using the DIII-D National Fusion Facility, a DOE Office of Science user facility, under Contract Nos. DE-SC0010685 and DE-FC02-04ER54698. This work was partly supported by National Natural Science Foundation of China under Grant Nos. 11775264 and 11575248. This work was sponsored in part by National Key R&D Program of China under Grant No. 2017YFE0300404. This work is also sponsored in part by Youth Innovation Promotion Association Chinese Academy of Sciences (2016384).

Disclaimer: This report was prepared as an account of work sponsored by an agency of the United States Government. Neither the United States Government nor any agency thereof, nor any of their employees, makes any warranty, express or implied, or assumes any legal liability or responsibility for the accuracy, completeness, or usefulness of any information, apparatus, product, or process disclosed, or represents that its use would not infringe privately owned rights. Reference herein to any specific commercial product, process, or service by trade name, trademark, manufacturer, or otherwise does not necessarily constitute or imply its endorsement, recommendation, or favoring by the United States Government or any agency thereof. The views and opinions of authors expressed herein do not necessarily state or reflect those of the United States Government or any agency thereof.

References

[1] Doyle E. J. *et al* 2007 *Nucl. Fusion* **47** S18
[2] Kinsey J. E. *et al* 2011 *Nucl. Fusion* **51** 083001
[3] Solomon W. M. *et al* 2014 *Phys. Rev. Lett.* **113** 135001
[4] Snyder P. B. *et al* 2015 *Nucl. Fusion* **55** 083026
[5] Ernst D. R. *et al* 2000 *Phys. Plasmas* **7** 615
[6] Manini A. *et al* 2006 *Nucl. Fusion* **46** 1047
[7] Snyder P. B. *et al* 2011 *Nucl. Fusion* **51** 103016
[8] Knolker M. *et al* 2019 Super H-mode: Optimizing the pedestal to greatly raise performance in future fusion reactors [JI2.00001] *61st Annual Meeting of the APS Division of Plasma Physics (Fort Lauderdale, USA, 2125 October 2019)* (http://meetings.aps.org/Meeting/DPP19/Session/JI2.1)
[9] Chrystal C. *et al* 2017 *Phys. Plasmas* **24** 042501
[10] Solomon W. M. *et al* 2013 *Nucl. Fusion* **53** 093033
[11] Politzer P. A. *et al* 2008 *Nucl. Fusion* **48** 075001
[12] Chang Z. and Callen J. D. 1990 *Nucl. Fusion* **30** 219
[13] Nave M. F. F. and Wesson J. A., 1990 *Nucl. Fusion* **30** 2575
[14] Jenko F. *et al* 2001 *Phys. Plasmas* **8** 4096
[15] Kotschenreuther M. *et al* 1995 *Phys. Plasmas* **2** 2381
[16] Romanelli F. 1989 *Phys. Fluids B* **1** 1018
[17] Hahm T. S. and Tang W. M. 1989 *Phys. Fluids B* **1** 1185
[18] Candy J. *et al* 2009 *Phys. Plasmas* **16** 060704
[19] Staebler G. M. *et al* 2007 *Phys. Plasmas* **14** 055909
[20] Belli E. A. *et al* 2012 *Plasma Phys. Control. Fusion* **54** 015015
[21] Meneghini O. *et al* 2015 *Nucl. Fusion* **55** 083008
[22] Staebler G. M. *et al* 2016 *Phys. Plasmas* **23** 062518
[23] Hughes J. W. *et al* 2018 *Nucl. Fusion* **58** 112003
[24] Citrin J. *et al* 2013 *Phys. Rev. Lett.* **111** 155001